DESIGN AND ANALYSIS OF A NEW MINIMALLY INVASIVE SPINAL CORD STIMULATION DEVICE

By

Luis Marquez

B.S, University of Alaska Fairbanks, 2018

Thesis

Submitted in partial fulfillment of the requirements for the Degree of Master of Science in the School of Engineering at Brown University

Providence, Rhode Island
May 2020

This thesis by Luis Marquez is accepted in its present form by the School of Engineering as satisfying the thesis requirements for the degree of Master of Science

Date: 04/30/20 Signature of Advisor: Vikas

Dr. Vikas Srivastava,

Assistant Professor of Engineering

Approved by the Graduate Council

Date: ____________ Signature of Dean: ____________

Dr. Andrew G. Campbell,

Dean of the Graduate School

Preface and Acknowledgments

I would like to thank my advisor Dr. Vikas Srivastava for allowing me to work in his lab and not only give me the opportunity to conduct research, but to let me grow as both a scholar and a person. I would also like to thank Savan Santoki, Sijun Niu, Yifei Bai, Zahra Ahmed, and the rest of the graduate and undergraduate for the countless fun we had in and outside of lab. Additionally I would like to thank Shailen Sampath for his assistance in the formulation of this thesis. Lastly I would like to thank my family, especially my Mom, for supporting me through all my odd endeavors.

Abstract

Shape memory polymers are polymers that respond to an environmental stimuli and can recover to their original shape from a stable temporary shape. They have the ability to recover from large deformations due to a wide range of stimuli in general. The types of stimuli range from electric, magnetic, pH, and temperature. In this thesis, the use of a bio-compatible and thermally responsive shape memory polymers in minimally invasive percutaneous spinal cord stimulation is investigated. This idea was originally conceived in detail by Dr. Vikas Srivastava and Dr. Albert Telfeian. This design increases coverage in the spinal column with the use of percutaneous leads that are smaller in diameter and requrie less invasive surgery. In our design, derived from the crosslinking between polymer chains, the properties of the shape memory polymer when coupled with the added stiffness of a super elastic metal alloy help bend various parts of the percutaneous leads. This design concept results in an increase in the dorsal region coverage of the spinal cord stimulus.

Table of contents

Contents

List of Tables

List of Figures

1 Introduction

1.1 Chronic Pain and Spinal Cord Stimulation

Chronic pain is a condition that affects about 1 in 5 Americans (Dahlhamer et al., 2018), in which 8% have high impact chronic pain, with the rates being higher among those with advanced age. There are many treatments for chronic pain, the most common being pain relievers. While effective, the most prevalent problem is the possible dependency and addiction that can arise while taking these, especially with opioids. This is reflected by the fact that 2.1 million Americans have some sort of opioid use disorder (Nathan, 2019).

Spinal Cord Stimulation (SCS) is an alternative to medicine that helps people with chronic pain, including back pain, nerve pain, complex regional pain syndrome, and visceral and abdominal pain. The objective in traditional SCS treatments is to mask the pain. While there is usually paresthesia associated with this treatment, recent advances having reduced or eliminated it altogether (Verrills, Sinclair, & Barnard, 2016). The leads are put into the posterior epidural space between the ligamentum flavum and dura mater (Figure1, 2, 2). The gap from these two points is around 5 millimeters in the lumber region, shrinking down to 2 in the sacrum region. The space from side to side in the space is approximately 15 mm in the lumbar region (Funct & Barolat, 1993).

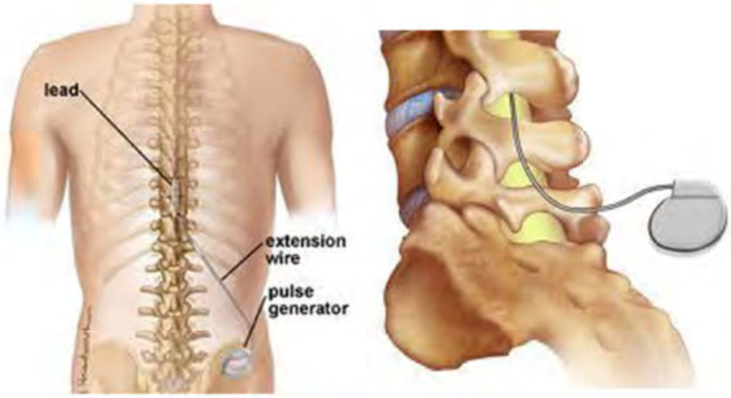

(a) Diagram of the leads and IPG

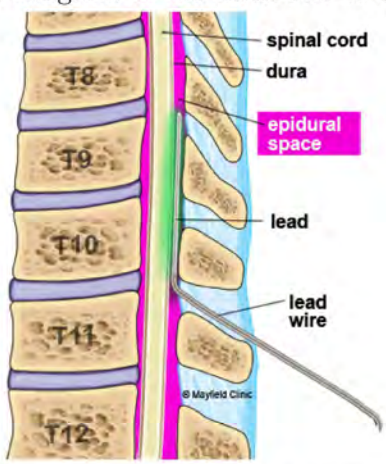

(b) Insertion of the lead into the epidural space

Figure 1: Percutaneous leads being inserted (Nichols, 2019)

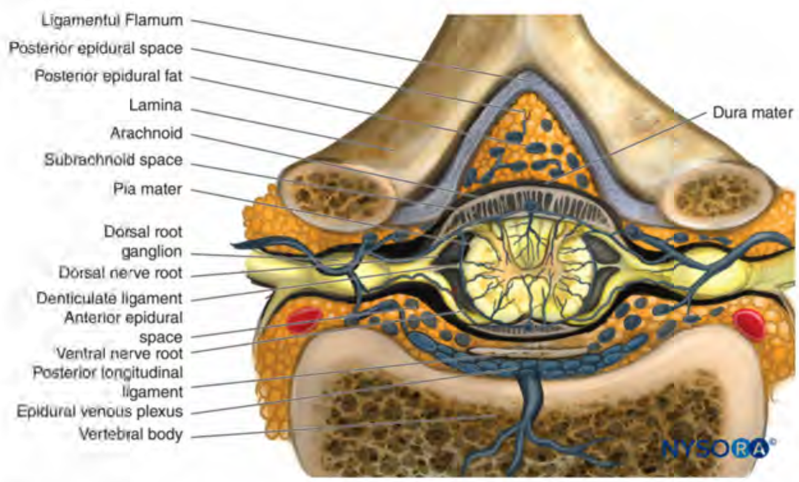

Figure 2: Top view of a vertebrae and the inside (de Velde & Toledano, 2008)

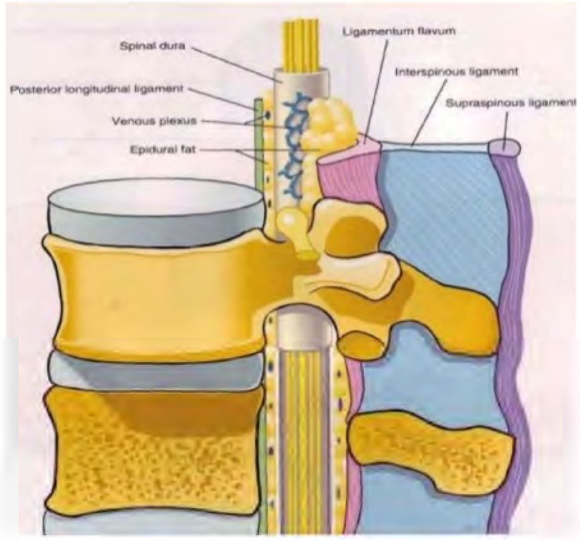

Figure 3: Side view of a vertebrae and the inside (Karzazi, 2014)

During the surgery, an incision is made in the middle of the back for lead insertion. A hollow needle (typically a 14 gauge surgical needle), just large enough to accommodate the percutanous, or cylindrical lead, is inserted into the epidural space utilizing the loss of resistance technique. Given that the epidural space consists of epidural fat and a small venous plexus, this technique is sufficient (Hawkins, 2011). In contrast, when inserting surgical, or paddle leads it requires either a laminectomy or laminotomy in order for the paddle lead to be inserted into the epidural space. By default, being able to use percutaneous leads leads to a less invasive surgery, with it having fewer complications and scar tissue that can develop (Behl & Lendlein, 2007).

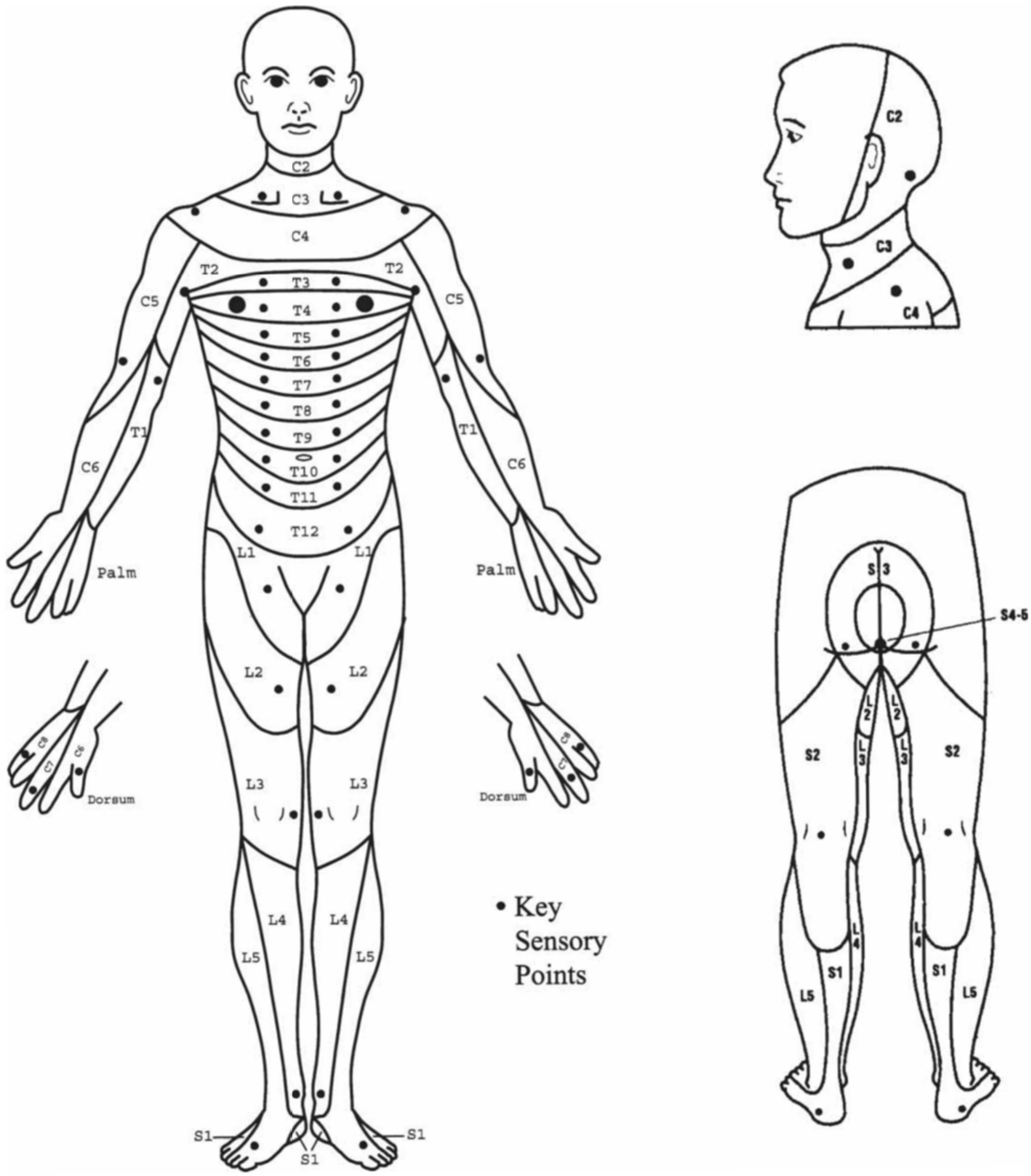

Figure 4: Relation between spinal vertebrae level and nerve input (Kirshblum et al., 2011)

Typically candidates for SCS go through a trial stage where the leads are implanted in the epidural space between the bone and the spinal cord. During this trial stage, the candidate will have an external generator that creates the electrical pulses. After 4 to 7 days of monitoring and logging activities including the kind of pain felt, the candidate will return to their doctor to discuss implanting the generator permanently (Implantable Pulse Generator or IPG), or removing it (Nichols, 2019). This period of logging activities and pain is important due to how the nerves innervate different regions of the body, which will dictate where the leads should be implanted. Figure 4 shows the relation between the nerve input in the spinal vertebrae. For the permanent implant the generator will be placed below the waistline (Figure 1a).

1.2 Thermoresponsive and Biocompatible Shape Memory Polymers

Shape memory materials, mainly shape memory metals, have been in use since the mid 1900's, where the memory effect is driven by the elastic behavior of the martensite phase. When factoring in weight and customizability, shape memory polymers come to the forefront of the field, given their rigidity, low weight, and characteristics being limited by the creativity of chemists. In addition to this, being able to tailor the biocompatability, biodegradability, and biostability of a polymer also makes them a more alluring and suitable option for biomedical purposes. Given the multitude of processes the body performs to keep everything functioning within a specific range (body temperature at 37°C, pH at 7.4, blood pressure at 120/80 mmHg or below, etc.), polymers are a good choice for challenges associated with working in the human body. These polymers can react to a wide variety of stimuli, ranging from temperature to pH (Chen et al., 2014) to electricity (Leng, Lv, Liu, & Du, 2008), and to magnetic fields (Ze et al., 2020).

Thermoresponsive shape memory polymers are a particular subset that change their shape depending on the temperature of its environment. Thermoset polymers, a subset of thermoresponsive SMP's which can start from a soft solid or a prepolymer, are cured through heat or some other sort of radiation such as UV light. This leads to a chemical reaction that creates thorough cross linking between the polymer chains from the precured material. These shaped memory polymers are able to recover a large deformation in a small form factor. To achieve a compacted state the polymer is heated to a point above its glass transition temperature (T_g) where it is a soft rubber-like material. Next the polymer is deformed to the desired shape and held in that position until it has sufficiently cooled, in which it can be thought to be in a temporary state. The shape memory polymer aspect is stimulated when the material is reheated somewhat close to the T_g and it returns to its original shape (Otsuka, 1998). The start of the vicinity of T_g is known as T_{onset}, where the polymer starts to regain some of its permanent shape, but slowly and it has not become rubber like yet. Typically, the closer the temperature is to T_g, the faster it will recover its shape.

2 Methods and Materials

2.1 Fabrication

The shape memory polymer (SMP) was made in house based off the paper by Yakacki et al., 2007 and Srivastava, Chester, & Anand, 2010 using Tert-butyl acrylate (tBA), poly(ethylene glycol)n dimethacrylate (PEGDMA), and photoinitiater 2,2- dimethoxy-2-phenylacetophenone, all purchased from Sigma-Aldrich. The constituents were 89.2%, 10%, and 0.2% by weight, respectively. SMP sheets were made via mold consisting of a petri dish bottom and cover made of glass slides, in which the solution, manually mixed and autoclaved for 10 minutes, was placed in between the two surfaces (Figure 5). This mold was separated by 1-2 spacers also made of glass slides, each 0.125 inches (3.175 mm) in thickness (Figure 6). Afterwards the solution was UV cured for 10 minutes at an intensity around 10 mW/cm^2 and oven cured for 60 minutes at 90°C. Once done the sheets are pulled off the glassware and any excess is cut off. Next, to cut out pieces of the SMP, the sheets are reheated and biopsy punches are used to cut our concentric rings, which are then cut in half and attached to a wire as hinges (Figure 7). These hinges were cut with an outer diameter of $\frac{3}{4}$" (19.05 mm) and inner diameter of $\frac{5}{8}$" (15.875 mm).

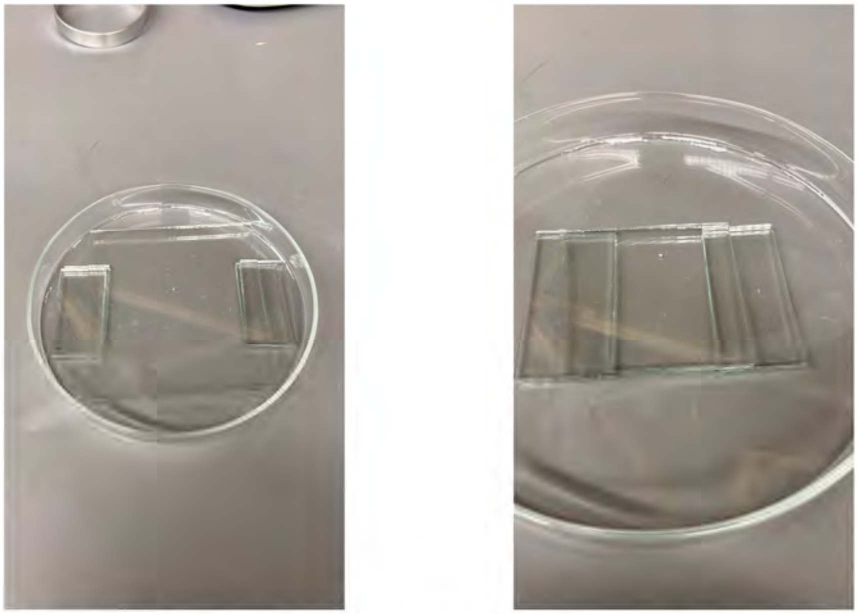

(a) Large set up for making shape memory polymer sheets

(b) Small set up for making shape memory polymer sheets

Figure 5: Set up of glass slides for making shape memory polymer sheets

(a) Thickness of a sheet sample, 0.25 in. (6.35 mm)

(b) Insertion of the lead into the epidural space

Figure 6: Small sample of a sheet made using slides

(a) Biopsy punches used to punch our the SMP hinges (b) Demonstrating the clarity of the SMP sheet

Figure 7: Punches and sample sheet

2.2 Properties

The properties of the PEGDMA shape memory polymer are driven by the cross-linking of the polymers in addition to the favored entropic and internal energy states that are preferred at it T_g (Liu & Mather, 2002). The properties of interest, true stress and true strain, graphed and shown below are taken from "Thermally actuated shape-memory polymers: Experiments, theory, and numerical simulations" (Srivastava, Chester, & Anand, 2010).

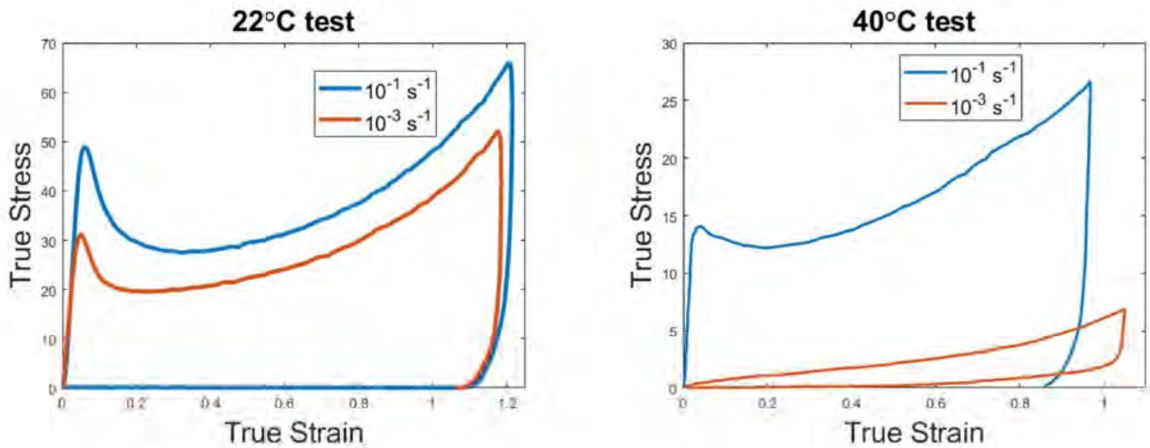

(a) Stress-strain curve at 22°C

(b) Stress-strain curve at 40°C

Figure 8: Stress-strain curves

Table 1: Initial Elastic Modulus at Different Temperatures (Room and Body) and Strain Rates (High and Slow)

Temperature (Celsius)	Strain Rate (s^{-1})	Young's Modulus (MPa)
22	10^-1	822.56
22	10^-3	622.00
40	10^-1	352.50
40	10^-3	6.57

3 Design of New System

3.1 Proof of Concept

In this thesis the use of shape memory polymers in minimally invasive percutaneous spinal cord stimulation is investigated, an idea that was originally conceived in detail by Dr. Vikas Srivastava and Dr. Albert Telfeian. The focus of this work is to both increase the electrodes that can be inserted as well as minimize the invasiveness of the ensuing surgery. To achieve this, the leads that are used will have to bend at certain points to give it an S shape, so as a proof of concept some polymer hinges were cut out from the polymer sheets made and then attached to a 34 gauge copper wire with super glue. Due to the chance of the glue adding another layer of material that the SMP would have to then bend once the glue cured, we only applied the glue to the ends of the polymer so that there were two contact points for the wire. As shown in Figure 9a, three 1 inch (25.4 mm) joints were used with about $\frac{1}{2}$ inch (12.7 mm) spacing. Once the SMP was heated up to 37°C (T_{onset}) in a temperature oven, the joints slowly started to regain their original shape over the course of 11 minutes, giving Figure 9b.

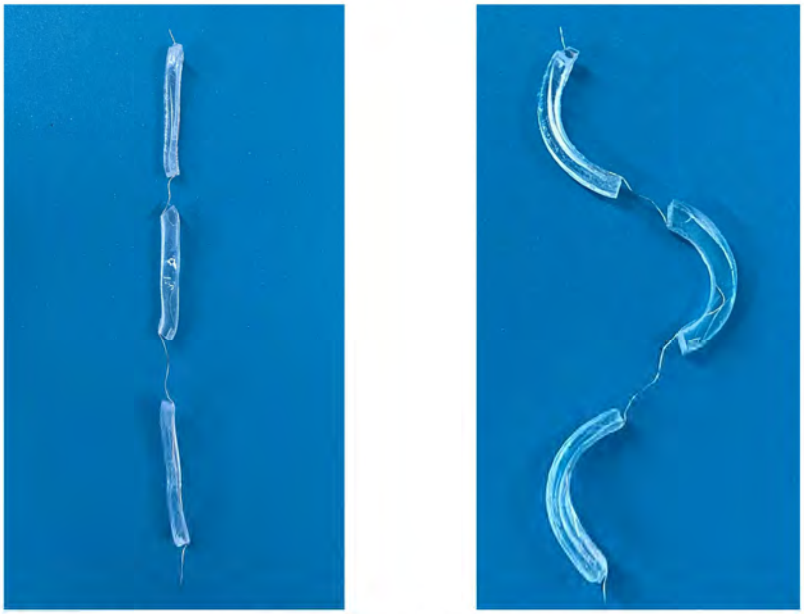

(a) Straight polymer joints at room temperature (24°C) (b) Curved polymer joints after heating at body temperature (37°C)

Figure 9: Polymer joints on wire before and after heating for 11 minutes

3.2 Design

As a starting point, leads from Boston Scientific were used given their reputation in the field of Spinal Cord Stimulation. The Infinion CX Lead with 16 electrodes was chosen for this study. Figure 10a shows some of the percutaneous leads that they offer with the leftmost schematic on Figure 10b showing the portion of the lead with the electrodes (gray) and the insulated spacers (black), which are 64 mm in total length. The middle schematic shows a lead that has a SMP hinge (red) on every other spacer. As shown, it can be seen that there are more electrodes in the same space, allowing for the initial surgery to only require a small incision. In contrast, paddle leads typically need a laminectomy in order to get more access to the spinal cord region, or in this case the epidural space. Typical percutanous leads are 1.3-1.4 mm in diameter (Boston Scientific, 2019; Abbott, 2017b) where as paddle leads are on average 500% wider (Boston Scientific, 2017; Abbott, 2017a) than the percutaneous leads at their widest, sitting around 4-10 mm with a thickness of 1.7-1.8 mm.

(a) Boston Scientific Percutenous Leads with varying quantity of electrodes and spacing (Boston Scientific, 2019)

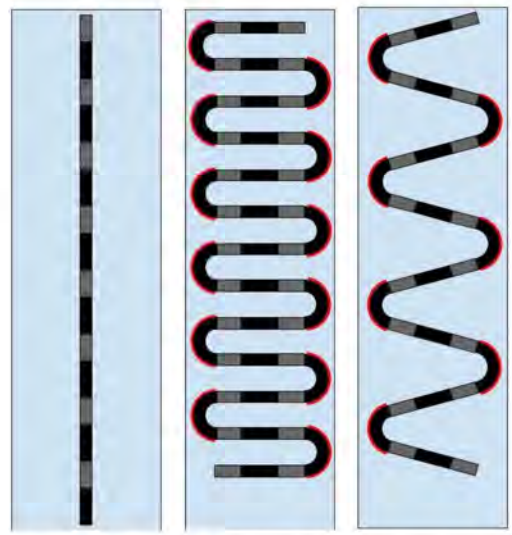

(b) (From left to right) schematic of straight leads, leads with semicircular bends, and leads with a arc bend, respectively

Figure 10: Percutaneous leads

Looking back at the middle schematic of Figure 10b we can see that having the hinges bend the spacers to have a 180° turn (semicircular curve), or radius of curvature ($R_{curvature}$) $= \frac{\text{arc length}}{4*\pi}$. If the SMP joints don't bend it all the way to that degree, there can still be some width left for the leads to take up, allowing for the possibility to add more electrodes in between the bends. This can further increase the amount of electrodes in the epidural space. In addition to the amount of space available in the epidural space, the 14 gauge needle also has to be taken into consideration when attaching these SMP joints.

The first objective is to calculate the amount of SMP we need in order to bend the lead. Following the proof of concept that was done, the SMP joints will be attached to the leads. Given the difference in stiffness between the platinum iridium (PtIr) wire and polyurethane coating, it is assumed that when considering the lead diameter, it is entirely the platinum iridium core. When comparing the stiffness of the SMP and the PtIr wire, it became apparent that more force was needed in order to bend the PtIr wire a sufficient amount from what was currently allowed within the 14 gauge needle. With this it was decided that an elastic metal alloy such as nitinol should be added to the SMP to increase its stiffness. This was calculated by comparing the bending stiffness of each SMP with a nitinol wire running through the middle and the PtIr wire. The bending stiffness used is in Eq(1), where E is Young's Modulus and I is second moment of inertia. As can be seen in Figure 11, the variables that can allow for a larger PtIr wire are the cross sectional base and height dimensions of the SMP: if the height decreases the PtIr can be thicker, and if the width decreases the SMP moves up, also allowing more vertical room for the PtIr.

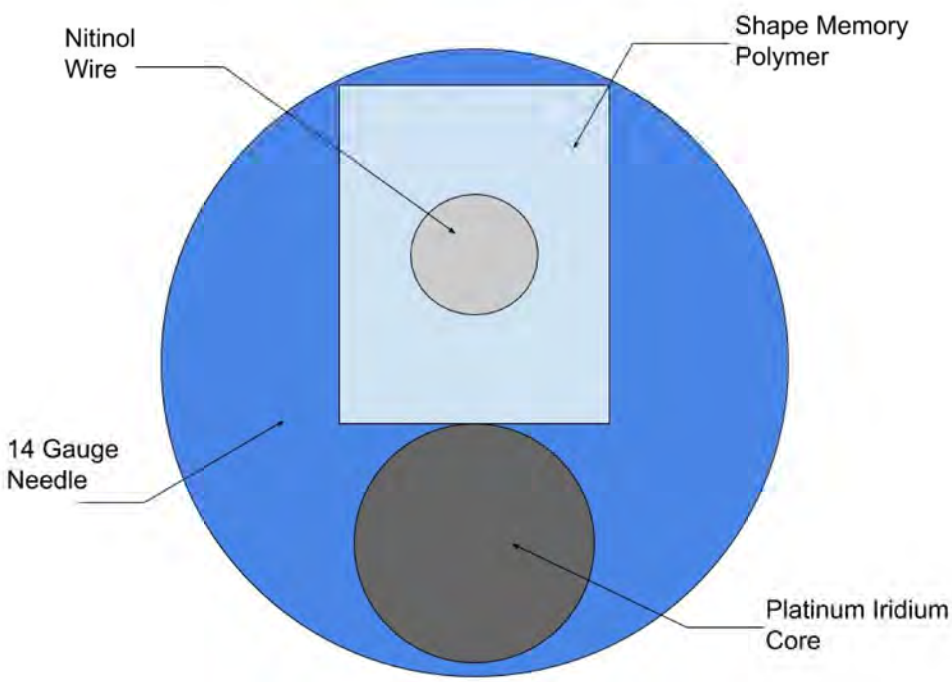

Figure 11: Cross sectional view of the proposed leads

The analysis used to find the dimensions of the PtIr core composed of using Eq. (1)

to analyze the radius of the nitinol wire needed given the cross-sectional dimensions of the SMP. For this we started out with a base of 0.6 mm and height of 0.6 mm. When calculating the second moment of inertia, the equations for a filled circle (Eq. (2)) and filled rectangle(Eq. (3)) were used, while utilizing the Young's Modulus values given in Table 2, with the nitinol values being taken from Šittner et al., 2014. Substituting the inertia values into stiffness and setting two stiffness equations equal to each other gives the radius of the PtIr core (r_{PtIr}). Note that the centroidal axis is not being used. This is because when looking at the radius of curvature the difference in the centroidal axis between the PtIr wire and the SMP/nitinol joint has to be considered, hence the $A * d^2$ term.

$$\kappa = E * I \tag{1}$$

$$I_{circle} = \frac{\pi}{4} * r_{nitinol}^4 + (A * d^2) = \frac{\pi}{4} * r_{nitinol}^4 + (\pi * r_{nitinol}^2 * (\frac{h}{2} + r_{PtIr})^2) \tag{2}$$

$$I_{rectangle} = \frac{b * h^3}{12} + (A * d^2) = \frac{b * h^3}{12} + (b * h * (\frac{h}{2} + r_{PtIr})^2) \tag{3}$$

Table 2: Young's Modulus for Metals

Material	Young's Modulus (GPa)
Nitinol at room temperature	66
Nitinol at body temperature	40
Platinum Iridium	165

Looking at Figure 10b, it is apparent that there are some constraints that dictate how many electrodes can be put into the given space. In the lumbar region of the spine where there is the most space, there is 15 mm available width and 64 mm for the height (Figure 12). Given this, there are two variables that are left to play with: arc length and radius of curvature for the SMP joints. In order to find how many electrodes can fit there must be constraints on the arc length, mainly having it come to a semicircular shape (Figure 10b). With this the range of the arc length can be between 0 and $R_{curvature}$ given a constant curvature. Alternatively, there can be a constant arc length and variable radius of curvature, but to start off the fixed variable will be the radius of curvature. First off, with a given radius of curvature and arc length, assuming that the arc length follows the path of a circle, we can find relative positions of the end points using the equation for arc length:

$$S = \int_a^b \sqrt{1 + \left(\frac{\partial y}{\partial x}\right)^2} dx = 2\int_0^b \sqrt{1 + \left(\frac{\partial y}{\partial x}\right)^2} dx \tag{4}$$

$$y = -\sqrt{R_{curvature}^2 - x^2} + R_{curvature}, \quad \frac{\partial y}{\partial x} = \frac{x}{\sqrt{R_{curvature}^2 - x^2}} \tag{5}$$

$$b = \sqrt{\frac{R_{curvature}^2(\tan\frac{S}{2R_{curvature}})^2}{1 + (\tan\frac{S}{2R_{curvature}})^2}} \tag{6}$$

From Eq. 4 it is seen that symmetry is used to reduce the variables to just solving for b, and in Eq. 6 we have the analytical solution for b with the symmetry assumption and that we are only solving for (Figure 13). However, when looking at the angle at which the electrode points at at the tip of the SMP joint, the angle there is less trivial to figure out. It turns out that that angle is:

$$\theta = \arctan\left(\frac{\partial y}{\partial x}\right) \tag{7}$$

From here it is assumed that there is only one electrode in between each SMP hinge i.e. one electrode in between every bend. Starting with this simple configuration another electrode can be added to see how many can fit into a given width. More specifically an electrode/spacer pair have to be added since there cannot be two electrodes together, since that makes an extra long electrode. With this given information of how many of these pairs can be added between each SMP joint, the total height can be calculated and from there the number of electrodes that can take up a given width and height can be calculated. To streamline calculations a script was written to add an electrode/spacer pair until the max width was taken up, and then find if the extra added electrode/spacer pairs could take up the available height. Figure 13 shows a simplified version of the leads, were we first take away any thickness, turning the leads into lines. From there we can add the diameter of the PtIr core with the SMP hinge attached to show much width the lead takes up to get a more accurate calculation.

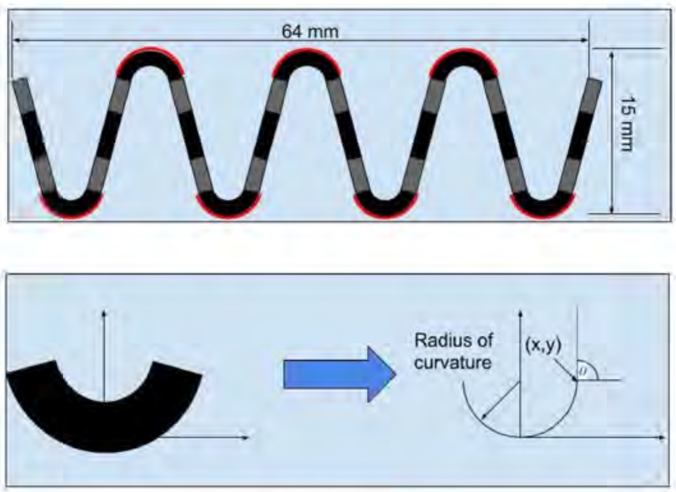

Figure 12: Simplifying the bending joints

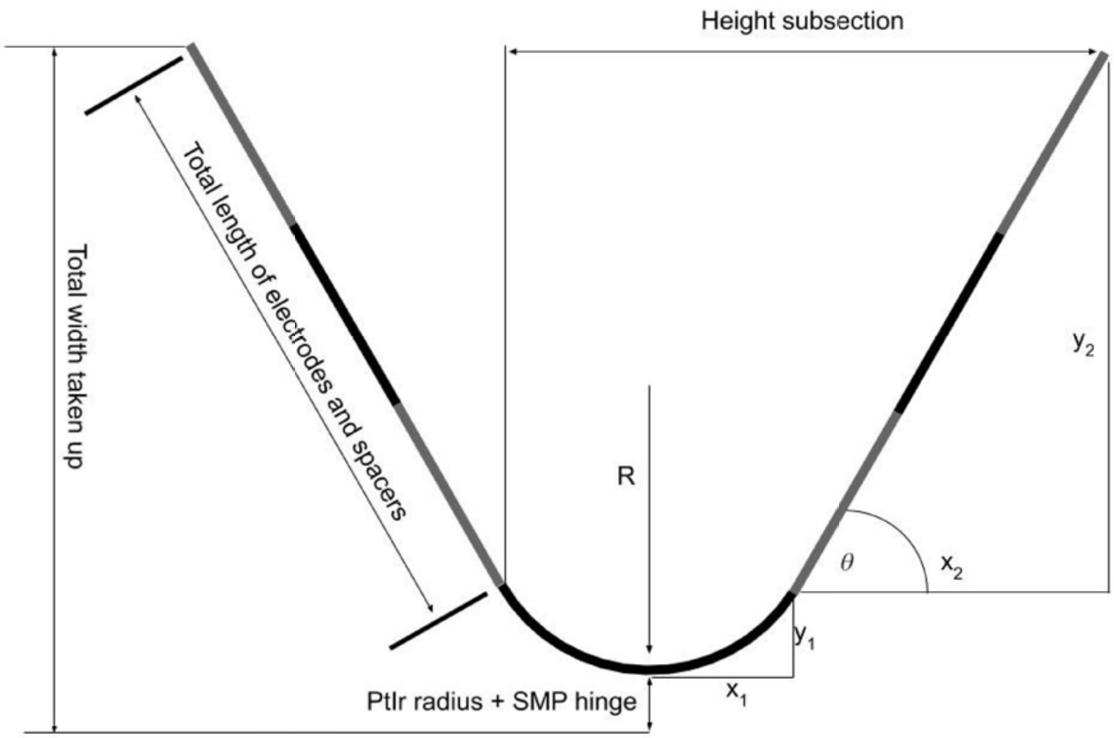

Figure 13: Simplifying the bending joints and electrode/spacers

Using these simplified models, the only variables are the radius of curvature and arc length the section of the lead that will be bending (S). A fixed radius of curvature of 3.2 mm and a varying arc length from 0 to $\pi R_{curvature}$ was used along with other constants as shown in Table 3. In Figure 14, it is observed that the best arc length is around 93% of the maximum allowed, which in this case is around 9.39 mm, giving a 12.5% increase in electrodes that can fit into the given space. From the Figure 14, it is observed that the amount of electrodes that can be fit into the space can vary by a large margin. The initial variations are due to the small bend of the hinges: if the electrode/spacer region is close to being vertical (Figure 10b) then there needs to be a larger number of electrode/spacer combinations in between each hinge to take up the allowable space width. When this happens, the straight regions of the leads are so long that it exceeds the allowable space height, leading to an inefficiency of how the space is being used up. When looking at the height subsection in Figure 13, we can see that this increases substantially when the arc length is small. By increasing this arc length the number of electrode/spacer combinations that can be added is decreased, but the height subsection is reduced.

Table 3: Final Dimensions of the Percutaneous Leads

Object	Value
Electrode length	3 mm
Edge to edge spacing	1 mm
SMP height	0.825 mm
SMP base	0.80 mm
Nitinol wire diameter	0.274 mm
Radius of curvature	3.2 mm
Arc length	9.39 mm
Electrodes per hinge	2
Platinum Iridium wire diameter	0.629 mm
Available total space height	64 mm
Available total space width	15 mm

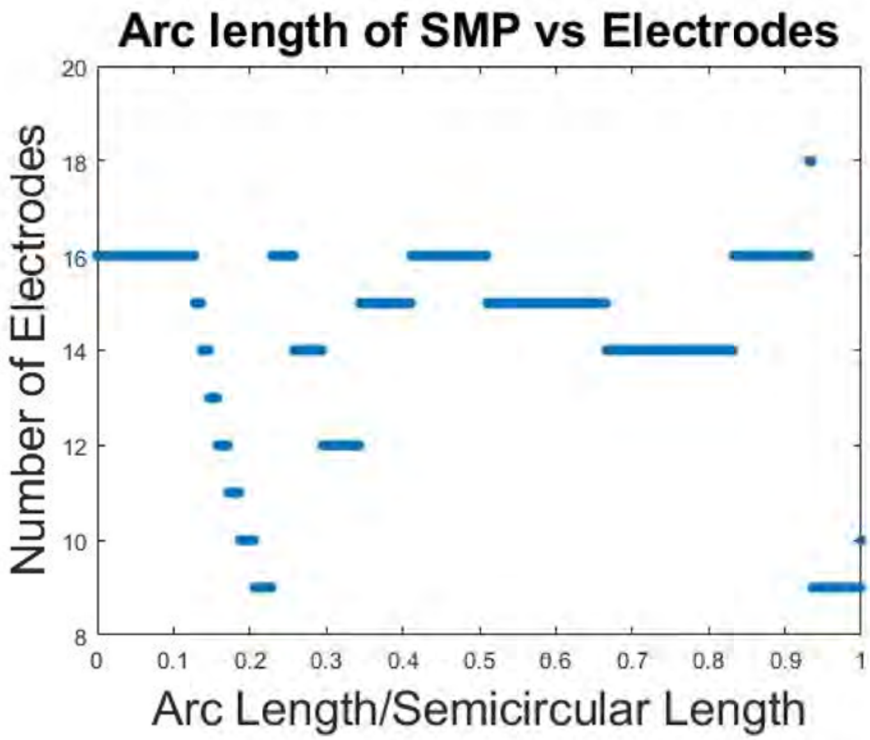

Figure 14: The normalized arc length vs electrodes that can be fit into a given area

4 Conclusion and Future Works

In this research project, use of shape memory polymers in minimally invasive percutaneous spinal cord stimulation is studied. A new design concept is optimized to allow incorporation of an optimum number of stimulus electrodes using minimally invasive surgical procedure. Given the increase in electrodes using percutaneous leads with the configuration calculated in this, our goal on increasing the number of electrodes has been achieved. The current configuration takes up almost all of the given space within the 14 gauge needle, which leads to a the question of how small can the PtIr core be so that a sufficient amount of current makes it to the electrodes. The current PtIr core diameter is proprietary information that isn't released to the public, so this had to be calculated. It is theorized that the current PtIr core diameter used in practice is more for keeping the leads rigid enough that they don't bend when inserting them into the epidural space. This leads to the assumption that the diameter of the core can then be reduced further which also reduces the size of the SMP hinge that is used. That being said, further refinements can be made in regard to other biocompatible shape memory polymers that can be studied. For a more accurate representation of a Spinal Cord Stimulation design finite element modeling and simulations can be performed, taking into account 3 dimensional movement and actual scale.

References

Abbott. (2017a). *Paddle Lead Kit Clinician's Manual.*

Abbott. (2017b). *Percutaneous Lead Kit.*

Behl, M., & Lendlein, A. (2007, apr). Shape-memory polymers. *Materials Today*, *10*(4), 20–28. doi: 10.1016/S1369-7021(07)70047-0

Boston Scientific. (2017). *Surgical Leads Directions for Use.*

Boston Scientific. (2019). *SCS Lead Portfolio - Boston Scientific.* Retrieved 2020-04-29, from `https://www.bostonscientific.com/content/gwc/en-EU/products/spinal-cord-stimulator-systems/scs{_}lead{_}portfolio.htmlhttp://www.bostonscientific.com/en-US/products/spinal-cord-stimulator-systems/scs{_}lead{_}portfolio.html`

Chen, H., Li, Y., Liu, Y., Gong, T., Wang, L., & Zhou, S. (2014). Highly pH-sensitive polyurethane exhibiting shape memory and drug release. *Polymer Chemistry*, *5*(17), 5168–5174. Retrieved from `www.rsc.org/polymers` doi: 10.1039/c4py00474d

Dahlhamer, J. M., Lucas, J., Zelaya, C., Nahin, R., Mackey, S., Debar, L., ... Helmick, C. (2018). *Prevalence of chronic pain and high-impact chronic pain among adults — United States, 2016* (Vol. 67; Tech. Rep. No. 36). Retrieved from `https://www.cdc.gov/nchs/nhis/index.htm.` doi: 10.15585/mmwr.mm6736a2

de Velde, M., & Toledano, R. D. (2008). *Epidural Anesthesia and Analgesia - NYSORA.* Retrieved 2020-04-13, from `https://www.nysora.com/regional-anesthesia-for-specific-surgical-procedures/abdomen/epidural-anesthesia-analgesia/`

Funct, S., & Barolat, G. (1993). *Original Paper Experience with 509 Plate Electrodes Implanted Epidurally from Cj to L* (Vol. 61; Tech. Rep.).

Hawkins, J. L. (2011, jan). Epidural analgesia and anesthesia. In *Anesthesia secrets* (pp. 458–465). Elsevier Inc. doi: 10.1016/B978-0-323-06524-5.00067-2

Karzazi, K. E. (2014). MR Imaging of spinal epidural lesions. In *European society of radiology.* doi: 10.1594/ecr2014/C-0354

Kirshblum, S. C., Burns, S. P., Biering-Sorensen, F., Donovan, W., Graves, D. E., Jha, A., ... Waring, W. (2011). *International standards for neurological classification of spinal cord injury (Revised 2011)* (Vol. 34) (No. 6). doi: 10.1179/204577211X13207446293695

Leng, J., Lv, H., Liu, Y., & Du, S. (2008, nov). Synergic effect of carbon black and short carbon fiber on shape memory polymer actuation by electricity. *Journal of Applied Physics*, *104*(10), 104917. Retrieved from `http://aip.scitation.org/doi/10.1063/1.3026724` doi: 10.1063/1.3026724

Liu, C., & Mather, P. T. (2002). Thermomechanical characterization of a tailored series of shape memory polymers. *Journal of Applied Medical Polymers*, *6*(2), 47–52.

Nathan, Y. (2019). *Addiction Statistics - Facts on Drug and Alcohol Use - Addiction Center.* Retrieved 2020-04-01, from `https://www.addictioncenter.com/addiction/addiction-statistics/`

Nichols, T. (2019). *Spinal cord stimulators, Spinal Cord Stimulation — Cincinnati, OH Mayfield Brain & Spine.* Retrieved from `https://mayfieldclinic.com/pe-stim.htm`

Otsuka, K. (1998). *Shape Memory Materials.*

Srivastava, V., Chester, S. A., & Anand, L. (2010). Thermally actuated shape-memory polymers: Experiments, theory, and numerical simulations. *Journal of the Mechanics and Physics of Solids*, *58*(8), 1100–1124. doi: 10.1016/j.jmps.2010.04.004

Verrills, P., Sinclair, C., & Barnard, A. (2016). A review of spinal cord stimulation systems for chronic pain. *Journal of Pain Research*, 9–481. Retrieved from `http://dx.doi.org/10.2147/JPR.S108884` doi: 10.2147/JPR.S108884

Ze, Q., Kuang, X., Wu, S., Wong, J., Montgomery, S. M., Zhang, R., ... Zhao, R. (2020). Magnetic Shape Memory Polymers with Integrated Multifunctional Shape Manipulation. *Advanced Materials*, *32*(4). doi: 10.1002/adma.201906657